

# Raman spectroscopy of graphene on different substrates and influence of defects<sup>†</sup>

ANINDYA DAS, BISWANATH CHAKRABORTY and A K SOOD\*

Department of Physics, Indian Institute of Science, Bangalore 560 012, India

**Abstract.** We show the evolution of Raman spectra with a number of graphene layers on different substrates, SiO<sub>2</sub>/Si and conducting indium tin oxide (ITO) plate. The *G* mode peak position and the intensity ratio of *G* and 2*D* bands depend on the preparation of sample for the same number of graphene layers. The 2*D* Raman band has characteristic line shapes in single and bilayer graphene, capturing the differences in their electronic structure. The defects have a significant influence on the *G* band peak position for the single layer graphene: the frequency shows a blue shift up to 12 cm<sup>-1</sup> depending on the intensity of the *D* Raman band, which is a marker of the defect density. Most surprisingly, Raman spectra of graphene on the conducting ITO plates show a lowering of the *G* mode frequency by ~6 cm<sup>-1</sup> and the 2*D* band frequency by ~20 cm<sup>-1</sup>. This red-shift of the *G* and 2*D* bands is observed for the first time in single layer graphene.

**Keywords.** Graphene; Raman spectroscopy; nano-carbon; phonons.

## 1. Introduction

The recent discovery (Novoselov *et al* 2004, 2005a, b; Zhang *et al* 2005) of thermodynamically stable two-dimensional single and bi-layer graphene has brought out many exciting experimental and theoretical studies, including the recent discovery of quantum Hall effect at room temperature (Novoselov *et al* 2007). The electronic properties near the Brillouin zone are governed by the Dirac equation, leading to the rich physics of quantum electrodynamics (Katsenelson and Novoselov 2007). The ballistic transport and high mobility (Novoselov *et al* 2005a; Zhang *et al* 2005) in graphene make it a potential candidate for future nano-electronic devices (Chen *et al* 2007; Han *et al* 2007; Lemme *et al* 2007). Furthermore, graphene is a building block for other carbon allotropes like nanotube and graphite and hence, its study will help in understanding the nanotubes.

Raman spectroscopy is one of the most powerful characterization techniques for carbon materials—be it three-dimensional form like diamond, graphite, diamond like carbon and amorphous carbon; two-dimensional graphene; one-dimensional carbon like nanotubes; and zero-dimensional carbon like fullerenes. Graphite has three most intense Raman features at ~1580 cm<sup>-1</sup> (*G* band), ~1350 cm<sup>-1</sup> (*D*-band) and ~2700 cm<sup>-1</sup> (2*D* band). A weak band at ~3248 cm<sup>-1</sup>, called 2*D'* band, is an overtone of *D'*

(1620 cm<sup>-1</sup>) mode. The *G* band is due to doubly degenerate *E*<sub>2g</sub> mode at the Brillouin zone centre, whereas *D* band arises from defect mediated zone-edge (near *K*-point) phonons. The 2*D* band originates from second order-double resonant Raman scattering from zone boundary, *K* + Δ*K* phonons. The intensity of the Raman 2*D* band can be finite even if the *D*-mode Raman intensity is negligible. It has been recently shown that Raman scattering can be used as a finger print for single, bi and a few layer graphene (Ferrari *et al* 2006; Gupta *et al* 2006; Graf *et al* 2007). Recent experiments also show that the phonon frequency of the *G* mode of graphene and longitudinal optical-*G* mode of metallic nanotube blue shifts significantly by both electron and hole doping achieved by electric field gating in a field effect transistor geometry (Lazzeri and Mauri 2006; Das *et al* 2007, 2008; Pisana *et al* 2007; Saha *et al* 2007; Yan *et al* 2007). In this paper, we present our work on the evolution of Raman spectra of the *G* and 2*D* modes for different graphene layers on Si/SiO<sub>2</sub> substrate. We will show that the *G* band peak position and *I*(*G*)/*I*(2*D*) ratio cannot be taken as a finger print to identify a single layer graphene. On the other hand, 2*D* Raman band shape and position are good finger prints of single and bilayer graphene to distinguish them from the multilayers. We also study the behaviour of the *G* peak frequency as a function of defects present in the single layer graphene, characterized by the intensity of the *D*-band.

Recently, there has been a debate about the minimal conductivity in graphene due to impurities present on the SiO<sub>2</sub> substrate (Adam *et al* 2007; Tan *et al* 2007). These impurities could be inhomogeneous charge puddles on the SiO<sub>2</sub> substrate. We will show that the signature of these impurities is manifested in a finite blue shift (~5–

\*Author for correspondence (asood@physics.iisc.ernet.in)

<sup>†</sup>Manuscript is based on the invited talk delivered at the National Review and Coordination Meeting on Nanoscience and Nanotechnology, 2007, Hyderabad, India.

$7 \text{ cm}^{-1}$ ) of the frequency of the  $G$  mode. It is, therefore, interesting to study the properties of graphene on different substrates. Here we report, for the first time, the Raman spectra of single and few layers graphene on the conducting indium tin oxide (ITO) plates. In contrast to  $\text{SiO}_2/\text{Si}$  substrate, the  $G$  mode frequency of the single and few-layer graphene on the ITO plate is red shifted ( $\sim 6 \text{ cm}^{-1}$ ) as compared to that of bulk HOPG ( $\sim 1580 \text{ cm}^{-1}$ ). A large softening ( $\sim 20 \text{ cm}^{-1}$ ) is also observed in the  $2D$  mode of the single and few-layer graphene on ITO as compared to the

graphene on  $\text{SiO}_2$  ( $\sim 2682 \text{ cm}^{-1}$ ). Such a lowering of frequency of the  $G$  as well as  $2D$  modes has not been reported so far.

## 2. Experimental

Graphene samples were prepared by micromechanical cleavage of bulk highly oriented pyrolytic graphite (HOPG) and were deposited on  $\text{SiO}_2/\text{Si}$  and transparent ITO plate. We adopted two methods to make the graphene samples. In method A, a small piece of HOPG was glued to a glass slide using photoresist as an adhesive (Novoselov *et al* 2004). Then a scotch tape was used to make the graphite flake thinner and thinner till no thicker graphite flake was visible on the glass slide. The next step was to transfer the thin flakes of graphite, almost invisible, from glass slide onto the  $\text{SiO}_2/\text{Si}$  substrate by dissolving the photoresist in acetone. Method B involved gentle pressing of the HOPG flake, adhered to a scotch tape, directly on top of a  $\text{SiO}_2/\text{Si}$  substrate, which left behind some thin graphene layers on the substrate. We used two different thicknesses of  $\text{SiO}_2$  (900 and 300 nm) on Si and found that 300 nm thickness gave more optical contrast to identify single

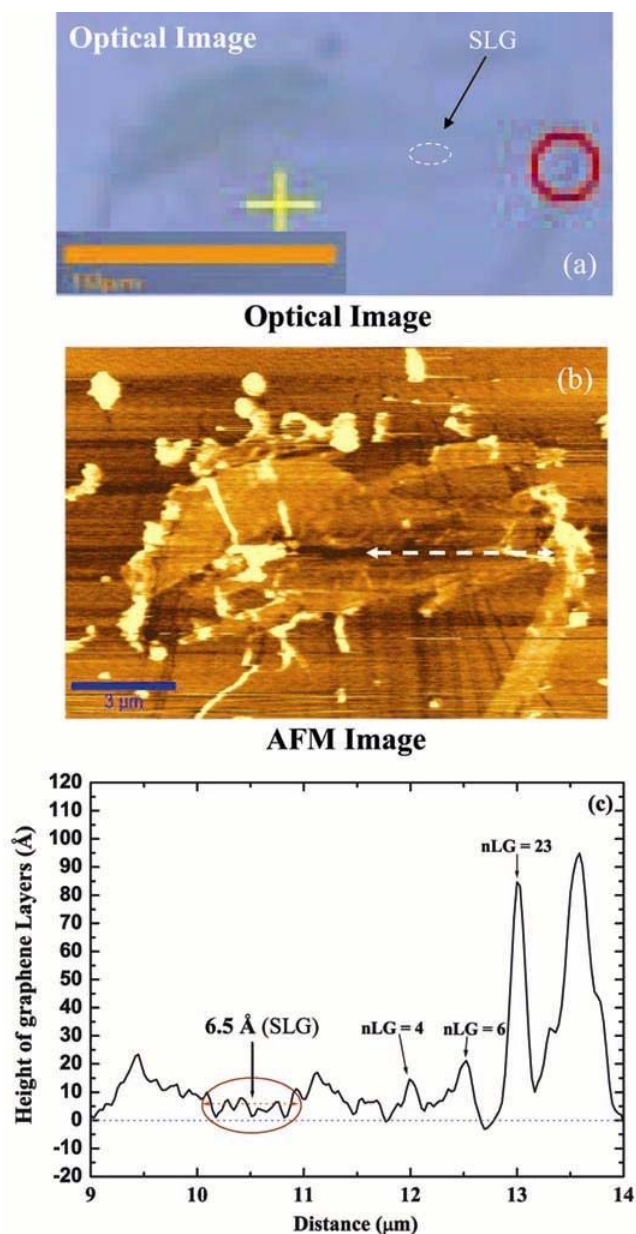


**Figure 1.** (Colour online). (a) Optical image of graphene flakes on 900 nm thick  $\text{SiO}_2/\text{Si}$ . The white marked region shows the single layer graphene (SLG), (b) AFM image of the above flake and (c) AFM line scan for height analysis along the white marked line in AFM image. SLG and nGL correspond to single and number of graphene layers, respectively.

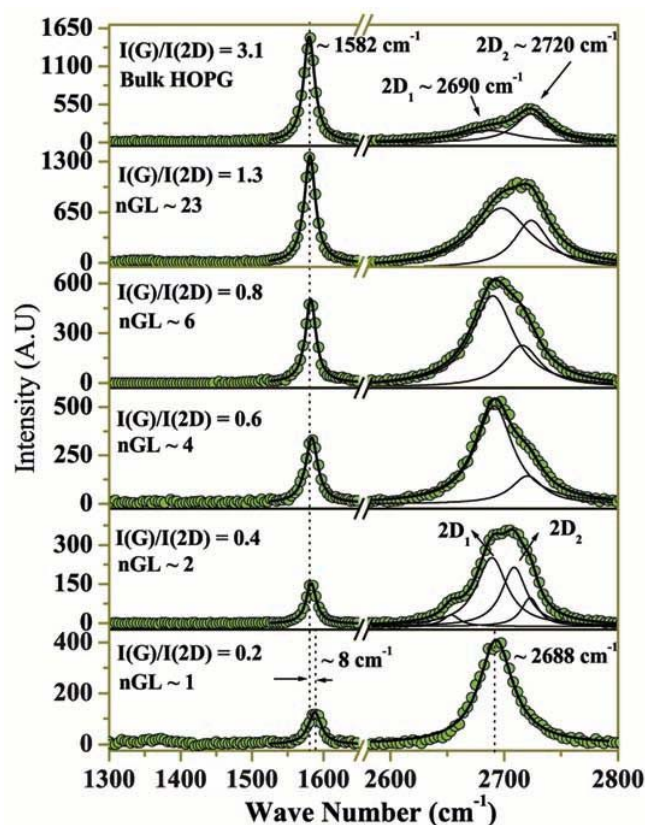


**Figure 2.** (Colour online). Raman spectra of  $G$  and  $2D$  mode for single, bi and few layers graphene. The open circles are the raw data and the solid lines are the fitted Lorentzian functions.

and bilayer graphenes (Casiraghi *et al* 2007). Among the two methods of sample preparation, we found that the method B produced better quality samples. Raman spectrum was recorded using WITEC confocal (X100 objective) spectrometer with 600 lines/mm grating, 514.5 nm excitation at a very low laser power level (<1 mW) to avoid any heating effect.

### 3. Results and discussion

We will divide the paper into three parts. In the first part, we will discuss Raman signatures of different layers of graphene using method A of preparation on SiO<sub>2</sub>/Si. In the second part, we will see the influence of defects on Raman spectra of single layer graphene using method A and compare them with the spectra from the samples prepared using method B. In the last part we will report the Raman spectra of different graphene layers on a conducting ITO plate.

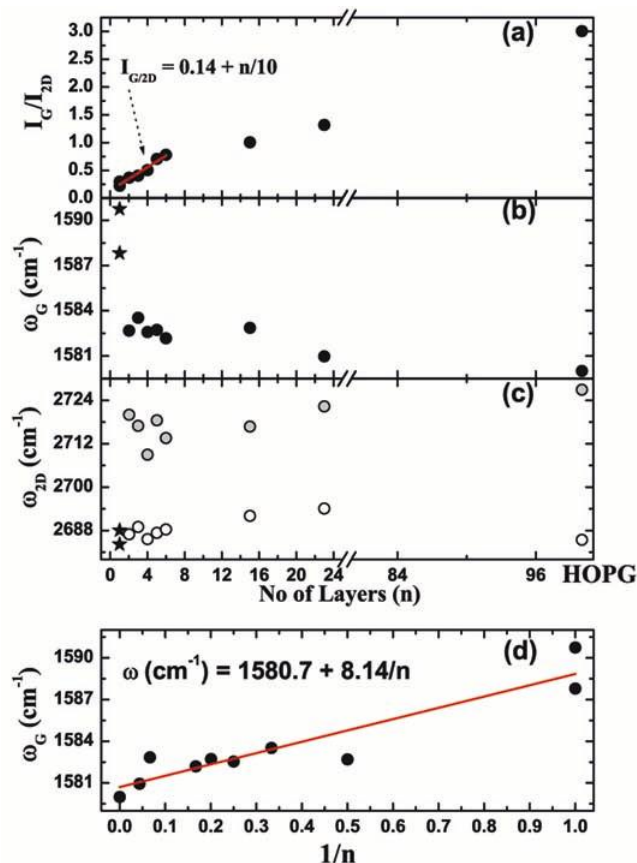


**Figure 3.** (Colour online). (a)  $I(G)/I(2D)$  intensity ratio as a function of graphene layers. Peak position of (b)  $G$  band and (c)  $2D$  band as a function of number of graphene layers (the stars correspond to the single  $2D$  component of SLG). (d)  $G$  band peak frequency as a function of inverse of graphene layers.

#### 3.1 Graphene on SiO<sub>2</sub>/Si

Figure 1a shows an optical image of graphene flake on 900 nm thick SiO<sub>2</sub>/Si substrate. The marked portion indicates the region of single layer. The optical contrast is poor for the graphene on 900 nm thick SiO<sub>2</sub>. To identify the single, bilayer and multilayer graphene, atomic force microscopy was used along with Raman spectroscopy. Figure 1b shows an AFM image of the graphene flake. The average height of the graphene layers is obtained from the AFM line scan analysis, as shown in figure 1c. In figure 1c, we notice that the roughness of the SiO<sub>2</sub>/Si substrate introduces noise in the height measurements. Due to different interactions of cantilever tip-substrate and cantilever tip-graphene, the height of single layer graphene is 0.6–0.7 nm for a single layer graphene, which is more than the van der Waal separation between SiO<sub>2</sub> and graphene (Gupta *et al* 2006).

Figure 2 shows Raman spectra (open circles) of different number of graphene layers, exhibiting  $G$  and  $2D$  modes. Solid lines are the Lorentzian fit to the data. It is seen that the intensity ratio of  $G$  and  $2D$  modes increases with the number of graphene layers. There is a blue shift of the  $G$  peak position ( $\sim 8$  cm<sup>-1</sup>) in single layer graphene compared to the bulk HOPG. The shape of the  $2D$  mode evolves significantly with the number of layers. The  $2D$  mode in bulk HOPG can be decomposed in two components,  $2D_1$  and  $2D_2$ , whereas single layer graphene has a single component. The  $2D$  Raman band in a bilayer is best fitted to four components. A single  $2D$  component in

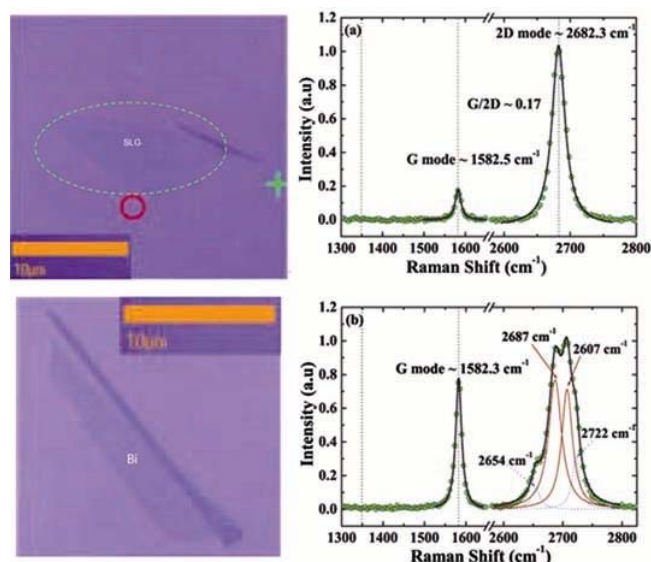


**Figure 4.** (Colour online). Raman spectra of a (a) single layer graphene and (b) bilayer graphene on 300 nm SiO<sub>2</sub>/Si using preparation method B. Optical images of single layer (top panel) and bilayer (bottom panel) graphene. Note that the  $D$ -band (expected near 1350 cm<sup>-1</sup>) is absent for both single and bilayer graphene.

monolayer and four components in bilayer graphene have been explained in terms of double resonance Raman scattering (Ferrari *et al* 2006), which invokes electronic structure of the graphene layers. Therefore, the electronic structure of graphene is captured in its 2D Raman spectra. Another interesting observation is that in bulk HOPG,  $2D_1$  component is less intense than the  $2D_2$  component, whereas, for the bilayer they have almost the same intensity and furthermore increase in the number of layers leads to an increment of intensity of the higher frequency,  $2D_2$  component compared to the  $2D_1$  component, as seen in figure 2.

In figure 3, we have plotted the  $I(G)/I(2D)$  intensity ratio,  $G$  peak position and  $2D$  peak position as a function of numbers of graphene layers. The  $I(G)/I(2D)$  ratio increases almost linearly up to 6–8 layers, as shown in figure 3a. For a single layer,  $I(G)/I(2D)$  intensity ratio is  $\sim 0.24$ , whereas for the bulk HOPG, it is  $\sim 3.2$ . The single layer graphene  $G$  mode appears at  $1590\text{ cm}^{-1}$ , whereas for the bulk HOPG it is at  $1580\text{ cm}^{-1}$ . Figure 3b shows that the  $G$  peak position shifts to higher frequency as the number of graphene layers decreases and it varies almost linearly with the inverse of number of graphene layers, as shown in figure 3d (also shown in Gupta *et al* (2006)). The single  $2D$  peak of the monolayer graphene appears at  $2685\text{ cm}^{-1}$  which is red shifted with respect to the  $2D_1$  ( $2690\text{ cm}^{-1}$ ) and  $2D_2$  ( $2720\text{ cm}^{-1}$ ) peak positions of the bulk HOPG.

### 3.2 Effects of defects

So far we have seen that the  $I(G)/I(2D)$  intensity ratio,  $G$  band peak position and the shape of the  $2D$  band evolve with the number of graphene layers on the  $\text{SiO}_2/\text{Si}$  sub-

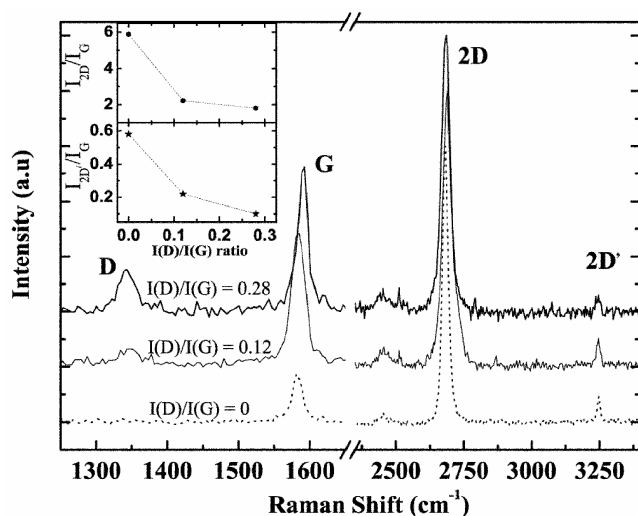


**Figure 5.** (Colour online). Raman spectra of single layer graphenes for different  $I(D)/I(G)$  values. Inset shows dependence of  $I(2D)/I(G)$  and  $I(2D')/I(G)$  on  $I(D)/I(G)$ .

strate using method A of preparation. Now we will look at the Raman spectra of the single layer graphene on  $\text{SiO}_2/\text{Si}$  using method B of preparation. Figure 4 shows that there is no shift in  $G$  peak position ( $\sim 1582\text{ cm}^{-1}$ ) of the single layer and bilayer graphene with respect to the bulk HOPG. Therefore,  $G$  peak position cannot uniquely identify the number of layers. It depends on how we prepare the samples. Recently, it has been shown that the  $G$  mode frequency increases as a function of both electron and hole doping (Pisana *et al* 2007; Yan 2007; Das *et al* 2008). The blue-shifted  $G$  peak position observed in graphene prepared by method A can, therefore, be attributed to unintentional doping in graphene by the charge impurities present on the  $\text{SiO}_2/\text{Si}$  substrate.

Another consequence of this unintentional doping is the presence of defects in single layer graphene. The defects could be edges, dislocations, cracks or vacancies in the sample. The so-called self-doping effects due to these defects are discussed in great detail by Castro Neto *et al* (Peres *et al* 2006; Castro Neto and Guinea 2007). They have predicted that the Raman frequency of the  $G$  mode should be

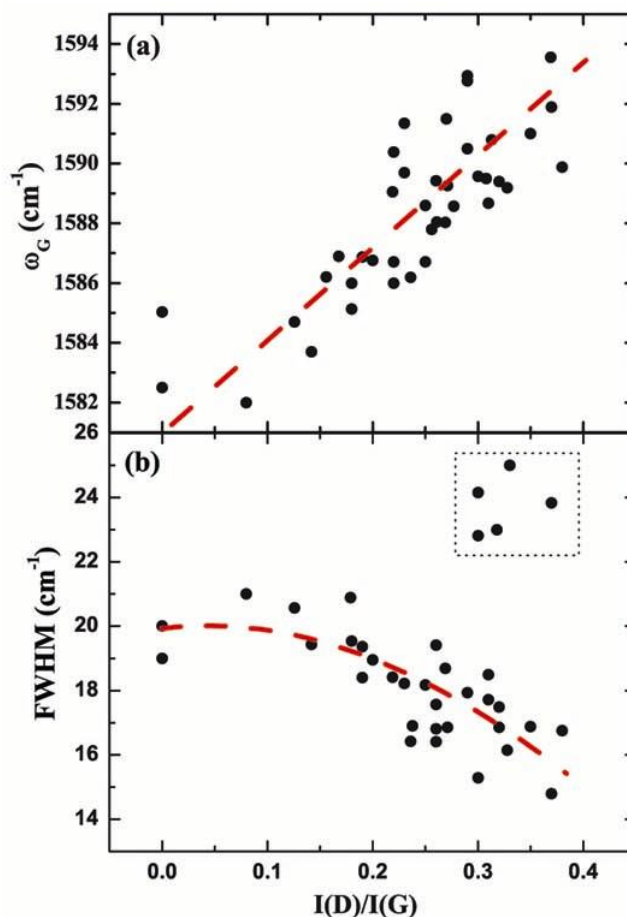


**Figure 6.** (Colour online). (a) Peak position and (b) FWHM of the  $G$  mode of different samples of single layer graphene as a function of  $I(D)/I(G)$  ratio. The dashed lines are guide to the eye.



larger in presence of defects. We have recorded the Raman spectra of several single layer graphene flakes. The amount of defects present in the sample can be quantified by measuring the intensity ratio ( $I(D)/I(G)$ ) of the  $D$  and  $G$  bands. Figure 5 shows Raman spectra of single layer graphenes which have different amounts of defects characterized by different  $I(D)/I(G)$  intensity ratios. We notice that the  $G$  band peak position increases with higher value of  $I(D)/I(G)$ . We also note that there is a decrease in intensity ratio of the  $I_{2D}/I_G$  and  $I_{2D}/I_G$  with more defects, as shown in the inset of figure 5. Figure 6 shows the  $G$

band peak position and FWHM as a function of  $I(D)/I(G)$  ratio for different single layer graphenes. The  $G$  frequency shift and decrement of FWHM are similar to the doping effects (Pisana *et al* 2007; Yan *et al* 2007; Das *et al* 2008). We note that for some graphene flakes, the FWHM is higher ( $\sim 24 \text{ cm}^{-1}$ ) with defects, as marked in a square box in figure 6b. This is opposite to the effect of doping, possibly due to the structural disorder as mentioned in Ferrari and Robertson (2001) and Casiraghi *et al* (2007b). As predicted by Castro Neto and Guinea (2007), we see that the  $G$  mode shifts almost linearly with defects. A maximum shift of the order of  $\sim 10 \text{ cm}^{-1}$  is observed, which corresponds to a self doping of  $\sim 10^{13} \text{ cm}^{-2}$ .

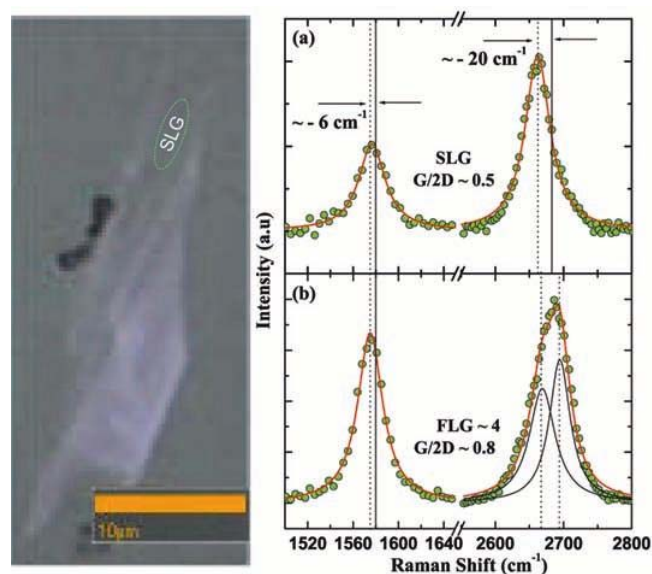


**Figure 7.** (Colour online). Left panel shows the optical image of a graphene flake on ITO. Raman spectra of (a) single layer graphene and (b) few-layers graphene on ITO plate.

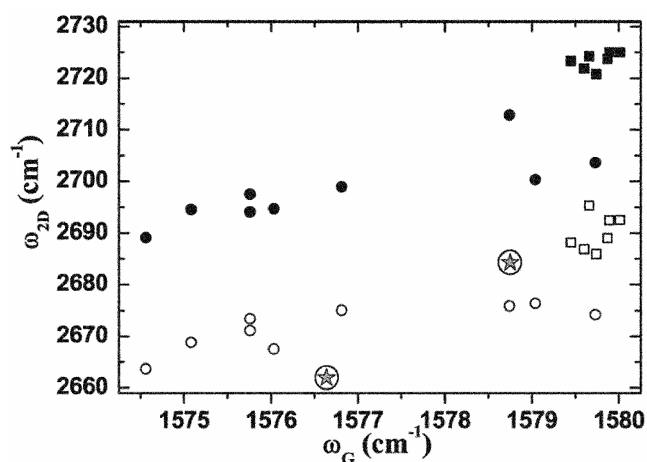


**Figure 8.** (Colour online).  $2D$  peak and  $G$  peak positions for single (stars inside a ring), a few layer (circles) and multilayer (squares) graphene on the ITO plate.

### 3.3 Graphene on conducting ITO plate

As we have discussed above, the charge impurities on  $\text{SiO}_2/\text{Si}$  substrate and defects play a major role in determining the position of the  $G$  band of a single layer graphene. Therefore, it is interesting to look at the Raman spectra of graphene flakes on a different substrate like conducting indium tin oxide coated glass substrate. The graphene flakes were transferred onto a conducting ITO substrate using preparation method A. The left panel of figure 7 shows an optical image of graphene flake on the ITO plate. The marked region shows a single layer portion, as identified by the  $2D$  Raman band. Optically it is very difficult to identify a single layer on the ITO plate, whereas we can see a colour contrast change for a few layers graphene. Figures 7a and b show the Raman spectra of a single layer and four-layer graphene on the ITO plate, respectively. The  $G$  and  $2D$  bands appear at  $1576 \text{ cm}^{-1}$  and  $2665 \text{ cm}^{-1}$ , respectively. It is interesting to note that the position of  $G$  and  $2D$  bands are red shifted by  $\sim 6 \text{ cm}^{-1}$  and  $\sim 20 \text{ cm}^{-1}$ , respectively compared to an undoped single layer graphene on the  $\text{SiO}_2/\text{Si}$  substrate. There is a correlation between the position of  $G$  and  $2D$  modes as shown in figure 8 which plots the position of  $G$  and  $2D$  modes of single layer (shown by stars inside a ring) and  $2D_1$  and  $2D_2$  modes of a few and multilayers graphenes. This is, to our knowledge, the first report of the red-shift of the  $G$  and  $2D$  modes of the single layer graphene as compared to the corresponding Raman spectra on  $\text{SiO}_2/\text{Si}$ . The origin of the red-shift is not yet fully understood. The lowering of the frequency implies that the unit cell constant of the graphene layer is enlarged when deposited onto the conducting ITO substrate. More studies are needed to understand the intriguing behaviour (red shift) of Raman spectra of graphenes on conducting ITO plate.

### Acknowledgement

One of the authors (AKS) thanks the Department of Science and Technology for funding the DST Unit in Nanoscience in IISc.

## References

- Adam Shaffique, Hwang E H, Galitski V M and Das Sarma S 2007 *cond-mat/0705.1540*
- Casiraghi C, Pisana S, Novoselov K S, Geim A K and Ferrari A C 2007 *cond-mat/0709.2566v1*
- Casiraghi C, Hartschuh A, Lidorikis E, Qian H, Harutyunyan H, Gokus T, Novoselov K S and Ferrari A C 2007 *Nano Lett.* **7** 2711
- Castro Neto A H and Guinea F 2007 *Phys. Rev.* **B61** 045404
- Chen Z, Lin Y M, Rooks M J and Avouris P 2007 *cond-mat/0701599*
- Das A, Sood A K, Govindaraj A, Saitta M, Lazzeri M, Mauri F and Rao C N R 2007 *Phys. Rev. Lett.* **99** 136803
- Das A *et al* 2008 *Nature Nanotech.* **3** 210
- Ferrari A C and Robertson J 2001 *Phys. Rev.* **B75** 14095
- Ferrari A C *et al* 2006 *Phys. Rev. Lett.* **97** 187401
- Graf D, Molitor F, Ensslin K, Stampfer C, Jungen A, Hierold C and Wirtz L 2007 *Nano Lett.* **7** 238
- Gupta A, Chen G, Joshi P, Tadigadapa S and Eklund P C 2006 *Nano Lett.* **6** 2667
- Han M Y, Ozyilmaz B, Zhang Y and Kim P 2007 *Phys. Rev. Lett.* **98** 206805
- Katsnelson M I and Novoselov K S 2007 *condmat/0703374v1*
- Lazzeri M and Mauri F 2006 *Phys. Rev. Lett.* **97** 266407
- Lemme M C, Echtermeyer T J, Baus M and Kurz H 2007 *IEEE Electr. Device Lett.* **28** 282
- Novoselov K S, Geim A K, Morozov S V, Jiang D, Zhang Y, Dubonos S V, Grigorieva I V and Firsov A A 2004 *Science* **306** 666
- Novoselov K S, Geim A K, Morozov S V, Jiang D, Katsnelson M I, Grigorieva I V, Dubonos S V and Firov A A 2005a *Nature* **438** 197
- Novoselov K S, Jiang D, Schedin F, Booth T J, Khotkevich V V, Morozov S V and Geim A K 2005b *PNAS* **102** 10451
- Novoselov K S, Jiang Z, Morozov S V, Stomer H L, Zeitler U, Maan J C, Boebinger G S, Kim P and Geim A K 2007 *Science* **315** 1379
- Peres N M R, Guinea F and Castro Neto A H 2006 *Phys. Rev.* **B73** 125411
- Pisana S, Lazzeri M, Casiraghi C, Novoselov K, Geim A K, Ferrari A C and Mauri F 2007 *Nature Mater.* **6** 198
- Saha S K, Waghmare U V, Krishnamurthy H R and Sood A K 2007 *cond-mat/0702627v2*
- Tan Y -W *et al* 2007 *cond-mat/0707.1807*
- Yan J, Zhang Y, Kim P and Pinczuk A 2007 *Phys. Rev. Lett.* **98** 166802
- Zhang Y, Tan Y -W, Stormer H L and Kim P 2005 *Nature* **438** 201